Photoplethysmographic Waveform Analysis for Autonomic Reactivity Assessment in Depression

Spyridon Kontaxis, Eduardo Gil, Vaidotas Marozas, Jesús Lázaro, Esther García, Mar Posadas-de Miguel, Sara Siddi, Maria Luisa Bernal, Jordi Aguiló, Josep Maria Haro, Concepción de la Cámara, Pablo Laguna, and Raquel Bailón

Abstract*—*Objective: **In the present study, a photoplethysmographic (PPG) waveform analysis for assessing differences in autonomic reactivity to mental stress between patients with Major Depressive Disorder (MDD) and healthy control (HC) subjects is presented.** ***Methods:*** **PPG recordings of 40 MDD and 40 HC subjects were acquired at basal conditions, during the execution of cognitive tasks, and at the post-task relaxation period. PPG pulses are decomposed into three waves (a main wave and two reflected waves) using a pulse decomposition analysis. Pulse waveform characteristics such as the time delay between the position of the main wave and reflected waves, the percentage of amplitude loss in the reflected waves, and the heart rate (HR) are calculated among others. The intra-subject difference of a feature value between two conditions is used as an index of autonomic reactivity.** ***Results:*** **Statistically significant individual differences from stress to recovery were found for HR and the percentage of amplitude loss in the second reflected wave (A_{13}) in both HC and MDD group. However, autonomic reactivity indices related to A_{13} reached higher values in HC than in MDD subjects (Cohen's $d = -0.81$, AUC $= 0.74$), implying that the stress response in depressed patients is reduced. A statistically significant ($p < 0.001$) negative correlation ($r = -0.5$) between depression severity scores and A_{13} was found.** ***Conclusion:*** **A decreased autonomic reactivity is associated with higher degree of depression.** ***Significance:*** **Stress response quantification by dynamic changes in PPG waveform morphology can be an aid for the diagnosis and monitoring of depression.**

***Index Terms*—Depression Monitoring, Stress Response, PPG Pulse Decomposition Analysis, Autonomic Nervous System, Arterial Stiffness**

This work was partly supported by projects RTI2018-097723-B-I00 funded by AEI and FEDER, LMP44-18 and Biomedical Signal Interpretation and Computational Simulation (BSICoS) group (T39-17R) funded by Gobierno de Aragón and FEDER, the European Union's Framework Programme for Research and Innovation Horizon 2020 (2014-2020) under the Marie Skłodowska-Curie Grant Agreement No. 745755, and the European Regional Development Fund (project No. 01.2.2-LMT-K-718-01-0030) under grant agreement with the Research Council of Lithuania (LMTLT). *Asterisk indicates corresponding author.*

* S. Kontaxis, E. Gil, J. Lázaro, P. Laguna,and R. Bailón are with BSICoS group at the Aragón Institute of Engineering Research (I3A), Instituto de Investigación Sanitaria de Aragón (IIS Aragón), University of Zaragoza, and CIBER in Bioengineering, Biomaterials & Nanomedicine (CIBER-BBN), Spain, (e-mail: sikontax@unizar.es).

V. Marozas is with Biomedical Engineering Institute and Department of Electronics Engineering, Kaunas University of Technology, Lithuania. E. García and J. Aguiló are with CIBER-BBN and Microelectronics and Electronic Systems Dept., Autonomous University of Barcelona, Spain. M. P. Miguel, M. L. Bernal are with IIS Aragón Zaragoza, Spain. S. Siddi is with CIBER de Salud Mental, Spain. J. M. Haro is with CIBER de Salud Mental and Parc Sanitari Sant Joan de Déu, Sant Boi de Llobregat, Barcelona, Spain. C. Cámara is with IIS Aragón Zaragoza and CIBER de Salud Mental.

I. Introduction

DEPRESSION is a serious mental disorder causing the affected person to suffer from sadness, loss of interest, poor concentration, and feelings of tiredness [1]. Major depressive disorder (MDD) is a leading cause of disability worldwide, and it has an enormous socioeconomic impact both due to the direct costs of treatment and the productivity losses associated to it [2].

MDD is a major contributor to the overall global burden of disease in combination with cardiovascular diseases [2]. Several studies indicate that both diseases may share underlying pathophysiological disturbances such as systemic inflammation, endothelial dysfunction, hypothalamic–pituitary–adrenal axis hyperactivity, and autonomic imbalance [3]–[5].

The link between psychological stress and depression can be found in the diathesis-stress model [6]. As the predisposition to depression (diathesis) increases, which can be attributed to either biological or psychological factors, a patient becomes psychologically more vulnerable, and thus the level of stress needed to precipitate an episode of depression decreases [7], [8]. Prolonged stress is a crucial factor underlying MDD considering that more than 40% of all depressed patients suffer from cooccurring anxiety. Negative emotions, such as depressive mood, could have adverse effects on neurohormonal regulatory circuits in a similar way to prolonged stress [3]. Thus, the comorbidity of anxiety and depressive disorders has been associated with poorer trajectories of depressive symptoms [9]. These observations highlight the need of assessing the individual variation in stress susceptibility, resilience, and reactivity [4].

In the short term, the physiological response to acute stress is associated with changes in the autonomic nervous system (ANS). The variation in ANS activity during stressful experiences, which is known as autonomic reactivity, is particularly important for adaptive stress responses, since it reflects the ability of an individual to cope with a challenging situation. Maladaptive responses may have a negative impact on cognitive, emotional, and behavioral processes, thereby leading to development of depression [10], [11]. Current research on stress response in MDD patients is focused on heart rate variability (HRV), which has been widely used for assessing ANS in a noninvasive way. Recent reviews have pointed out that individuals with greater levels of resting HRV have greater emotion regulation and executive functioning, while hypo-reactivity during stress, evidenced by blunted HRV

reactivity, is related to depression [12], [13].

Although autonomic reactivity in MDD patients using HRV indices derived from the electrocardiogram (ECG) has been widely investigated, the use of photoplethysmography (PPG) in this application remains largely unexplored. In [14], MDD patients showed a reduced high frequency component of the pulse rate variability (PRV) compared to healthy control subjects during a stressful stimuli. Similar results were reported by [15], where HRV indices derived from a PPG signal were studied before, during, and after executing a mental task.

However, a PPG signal does not only contain information about heart rate (HR). Pulse pressure propagation in arteries causes alterations in blood volume and accordingly changes in the PPG pulse shape and temporal characteristics [16]. Thus, PPG can provide a great amount of information about the cardiovascular system including autonomic function and vascular characteristics. One of the very few studies involving MDD patients investigated the association between autonomic dysregulation and arterial stiffness measured by PPG waveform characteristics but only during resting conditions [17].

The novelty of the present study consists in the use of morphological PPG changes for assessing autonomic reactivity induced by cognitive tasks in MDD and healthy subjects. Pulse waveform characteristics are calculated based on a pulse decomposition analysis (PDA) that consists of modeling the PPG pulse as a main wave superposed with several reflected waves [18]. The main hypothesis tested in the present study is that the stress response quantified by dynamic changes in vascular characteristics is useful for the diagnosis and monitoring of depression.

II. Materials

A. Participants

A database of 40 MDD patients (white males and females) recruited from consultation as well as from the psychiatric inpatient ward was recorded at the Hospital Clínico Lozano Blesa (Zaragoza, Spain) and the Mental Health Unit of the Parc Sanitari Sant Joan de Deú (Barcelona, Spain). The MDD group consists of subjects with clinically significant depression. The selection was based on the diagnostic and statistical manual of mental disorders (DSM-5) [19]. Depression severity was assessed with the Hamilton depression rating scale (HDRS) [20] and the Beck's depression inventory-II (BDI) [21]. Recordings of 40 healthy control (HC) subjects matched by age, sex, race, and body mass index (BMI) were acquired. Only participants without other comorbidities such as cardiovascular, endocrinological or neurological disorders were selected. Table I shows the demographic data and medication of the subjects.

TABLE I
Demographic data (mean±SD) and medication of the participants

	MDD	HC	
Number of subjects	40	40	
Female subjects	24	24	
Unmedicated subjects	3	40	
Subjects with AD and BZ	26	0	
Subjects with only AD	7	0	
Subjects with only BZ	4	0	
Age (years)	45.4 ± 13.35	44.3 ± 12.2	n.s.
BMI (kg/m^2)	27.14 ± 5.16	24.78 ± 4.64	n.s.
HDRS	22.2 ± 6.5	2.1 ± 2.6	**
BDI	27.5 ± 12.2	3.7 ± 3.7	**

* $p < 0.01$, ** $p < 0.001$, n.s. not significant; AD: Antidepressants, BZ: Benzodiazepines

B. Experimental protocol and data acquisition

The experimental protocol had a duration of about 2 hours (starting time between 09:00 a.m. and 11:00 a.m. to avoid circadian rhythm changes) and it consists of three stages. The first stage consists in a basal condition ($\mathcal{B}$), where the subjects were filling psychometric tests including state-trait anxiety inventory test, scale of stress symptoms, perceived stress scale, and visual analogue stress scale [22].

Then, in the second stage, stress was induced to participants by applying two cognitive tasks widely-used in the neuropsychological field for assessing executive function: first the trail making test ($\mathcal{S}_{\mathrm{T}}$) followed by the stroop color task ($\mathcal{S}_{\mathrm{C}}$), consisting in a non-verbal and verbal stressor, respectively [23], [24]. The $\mathcal{S}_{\mathrm{T}}$ consists of two parts. In Part A, the subjects are required to connect, by drawing a line, consecutive numbers, while in Part B, they are required to connect numbers and letters in an alternating progressive sequence. In $\mathcal{S}_{\mathrm{C}}$, subjects are required to read, as fast as possible in 45 secs, from three different lists, the names of: (a) color-words printed in black ink, (b) different color patches, (c) ink color of color-words printed in an inconsistent color ink (incongruent condition).

In the third stage, subjects were requested to relax and to remain silent. During this recovery stage ($\mathcal{R}$), of about 5 minutes, individuals were supposed to achieve a resting state.

The duration (mean±SD) of each protocol stage was 11.5 ± 5.0 min ($\mathcal{B}$), 3.5 ± 1.4 min ($\mathcal{S}_{\mathrm{T}}$), 4.3 ± 1.2 min ($\mathcal{S}_{\mathrm{C}}$), 5.2 ± 0.5 min ($\mathcal{R}$). During the whole experimental protocol, a non-dominant hand fingertip PPG signal was continuously recorded at a sampling frequency of 250 Hz for each participant using the Medicom system (ABP10 module of Medicom MTD, Ltd, Russia).

This study was carried out in accordance with the recommendations of "Comité Ético de Investigación Clínica de Aragón (CEICA)" and the Ethical Committee of "Fundació Sant Joan de Déu" under clinical studies PI16-0156 and PIC-148-16, respectively, including written informed consent from all subjects in accordance with the Declaration of Helsinki.

III. Methods

A. Pulse decomposition analysis

Intervals of the PPG signal containing artifacts are suppressed using the energy-based approach proposed in [25]. Then, PPG pulse detection is carried out using a low-pass differentiator (transition band from 7.7 Hz to 8 Hz) and a time-varying threshold [26]. For the i:th pulse, the fiducial point $n_{\mathrm{F}}(i)$ consists in the maximum up-slope point of the low-pass differentiator filtered signal.

A pulse decomposition analysis (PDA) technique based on [18] is applied for pulse waveform modeling. Prior to PDA,

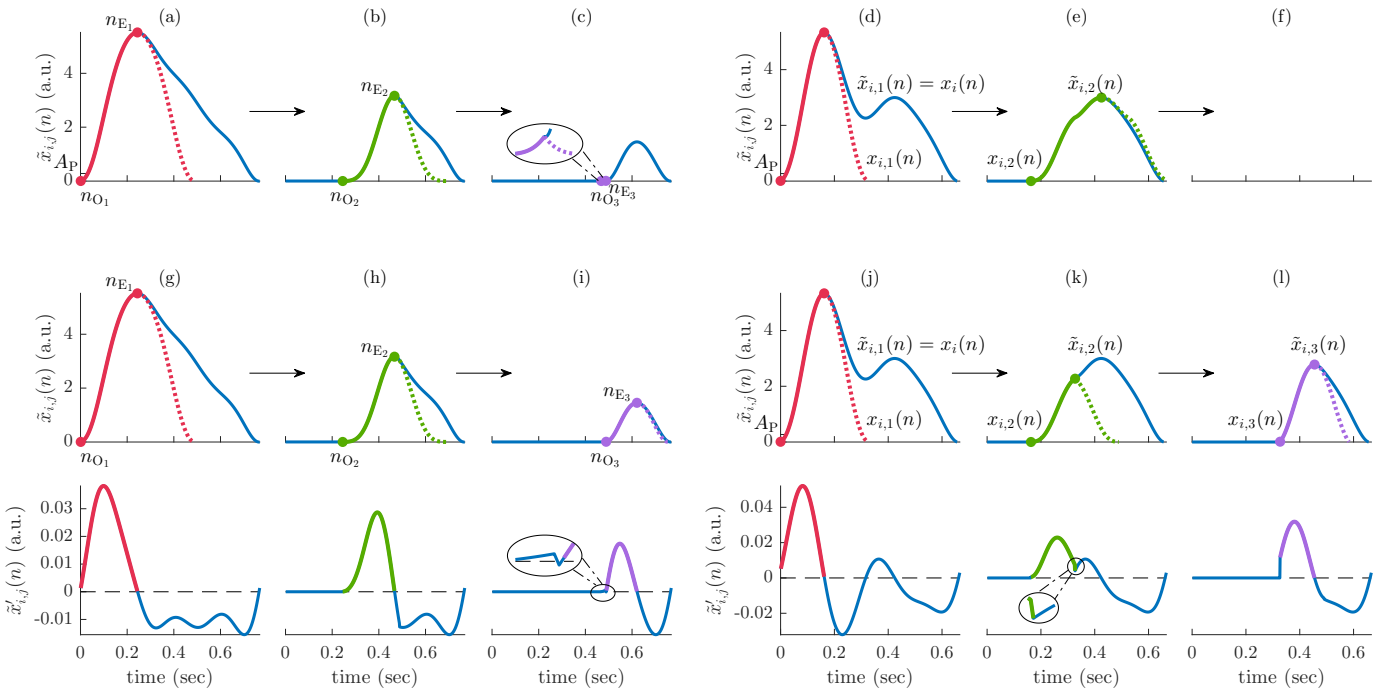

Fig. 1. Pulse decomposition algorithm. Recursive computation of inner waves for two different pulse morphologies of $x_i(n)$ in (a)-(c), and (d)-(f). (g)-(l) The result of decomposition for the same pulse morphologies taking into account the first derivative of the running residual $\tilde{x}_{i,j}(n)$ ($\tilde{x}'_{i,j}(n)$). The inner waves $x_{i,1}(n)$, $x_{i,2}(n)$, $x_{i,3}(n)$ are marked in red, green, and purple, respectively; the up-slope is marked with solid line, while the horizontally flipped up-slope with dashed line.

the raw PPG signal is subjected to low-pass filtering (forth order bidirectional IIR with cut-off frequency of 5 Hz) for attenuating high frequency noise, with $x_{\text{PPG}}(n)$ denoting the filtered signal. In this study, due to low-pass filter operations, a percentage relative to the maximum up-slope value of the first derivative of $x_{\text{PPG}}(n)$ ($x'_{\text{PPG}}(n)$) is used for defining the pulse basal point ($n_{\text{B}}(i)$). The point $n_{\text{B}}(i)$ is searched in the interval $\mathbf{\Omega} = [n_{\text{U}}(i) - 0.3F_s, n_{\text{U}}(i)]$ around the maximum up-slope point of $x'_{\text{PPG}}(n)$ ($n_{\text{U}}(i)$):

$$n_{\text{B}}(i) = \underset{n\in\mathbf{\Omega}}{\arg\min} \left\{ |x'_{\text{PPG}}(n) - 0.05 \cdot x'_{\text{PPG}}(n_{\text{U}}(i))| \right\}, \quad (1)$$

where $x'_{\text{PPG}}(n) = x_{\text{PPG}}(n) - x_{\text{PPG}}(n-1)$. The point $n_{\text{U}}(i)$ is defined as the absolute maximum of $x'_{\text{PPG}}(n)$ in a symmetrical fixed window of 10 msec around the time instant associated with $n_{\text{F}}(i)$. Linear interpolation of $x_{\text{PPG}}(n_{\text{B}}(i))$ series is subtracted from $x_{\text{PPG}}(n)$, yielding $\check{x}_{\text{PPG}}(n)$. Thus, each pulse $x_i(n)$ begins and ends with zero amplitude:

$$x_i(n) = \check{x}_{\text{PPG}}(n + n_{\text{B}}(i)) \quad n \in [0, \ldots, n_{\text{B}}(i+1) - n_{\text{B}}(i)]. \quad (2)$$

The i:th pulse wave $x_i(n)$ is decomposed into J symmetrical waves $x_{i,1}(n), \ldots, x_{i,\text{J}}(n)$, and a residual signal. The j:th inner wave $x_{i,j}(n)$ is obtained by concatenating the up-slope of the running residual signal $\tilde{x}_{i,j}(n)$ ($\tilde{x}_{i,1}(n) = x_i(n)$) with itself horizontally flipped, assuming that the reflected waves arrive after half of the incident pulse is over:

$$x_{i,j}(n) = \begin{cases} \tilde{x}_{i,j}(n), & n \in [n_{\text{O}_j}, n_{\text{E}_j}], \\ \tilde{x}_{i,j}(-n + 2n_{\text{E}_j}), & n \in (n_{\text{E}_j}, 2n_{\text{E}_j} - n_{\text{O}_j}], \\ 0, & \text{otherwise}, \end{cases} \quad (3)$$

where n_{O_j} and n_{E_j} denote the up-slope onset and end of $\tilde{x}_{i,j}(n)$, respectively; the dependence of i in the up-slope onset n_{O_j} and end n_{E_j} is omitted for simplicity. After the up-slope interval has been defined, the j:th inner wave $x_{i,j}(n)$ is subtracted from the running residual $\tilde{x}_{i,j}(n)$, i.e., $\tilde{x}_{i,j+1}(n) = \tilde{x}_{i,j}(n) - x_{i,j}(n)$, and the $(j+1)$:th inner wave is computed recursively from $\tilde{x}_{i,j+1}(n)$; J is set to 3.

Figure 1 illustrates an example of PDA for two different pulse waveform morphologies. The up-slope end n_{E_j} is the position of the first relative maximum of $\tilde{x}_{i,j}(n)$ and the up-slope onset n_{O_j} ($n_{\text{O}_j} < n_{\text{E}_j}$) is the first non-negative-amplitude sample of $\tilde{x}_{i,j}(n)$ [18], e.g., for the main wave $n_{\text{O}_1} = n_{\text{B}}$ (see Fig. 1(a)). However, relative maxima with low amplitude (see Fig. 1(c)), can lead to erroneous definition of inner waves. Thus, in this work, an inner wave is considered to exist only if the absolute maximum value of $\tilde{x}_{i,j}(n)$, i.e., $\tilde{x}_{i,j}(n_{\text{E}_j})$, exceeds the fixed (for the i:th pulse) amplitude threshold $A_{\text{P}} = 0.05 \cdot \max_n \{x_i(n)\}$.

Furthermore, slope changes prior to the first relative maximum can lead to erroneous decomposition (see Fig. 1(e)). When $x_i(n)$ is decomposed to inner waves, the up-slope of the running residual $\tilde{x}_{i,j}(n)$ might not be a strictly increasing function in $[n_{\text{O}_j}, n_{\text{E}_j}]$, i.e., the first derivative of $\tilde{x}_{i,j}(n)$ $(\tilde{x}'_{i,j}(n))$ is not always positive (see Fig. 1(i)) or has more than one inflection points (see Fig. 1(k)). This is either due to the presence of a relative maximum with amplitude lower than A_{P} at the beginning of the up-slope interval (see Fig. 1(i)), or due to a slope change at the end of up-slope interval which, however, does not appear as a relative maximum in $\tilde{x}_{i,j}(n)$ (see Fig. 1(k)). Thus, n_{O_j} is redefined as the next sample after the last negative-amplitude sample of $\tilde{x}'_{i,j}(n)$, so that $\tilde{x}'_{i,j}(n) \geq 0$. Then, n_{E_j} is redefined as the position of the

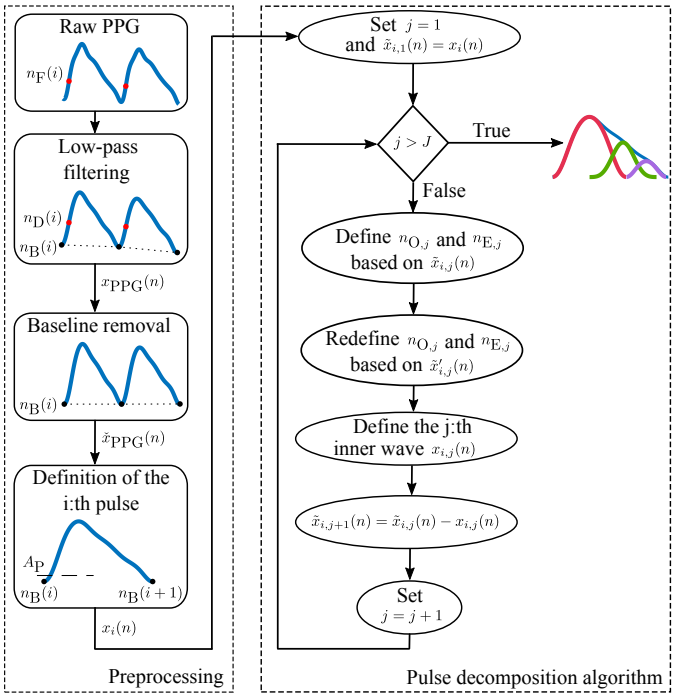

Fig. 2. Block diagram of the pulse decomposition algorithm.

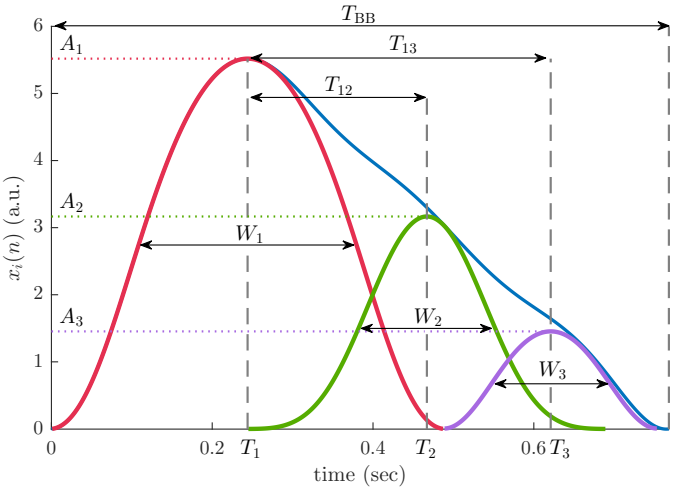

Fig. 3. Pulse waveform characteristics. Morphological features derived from amplitude A_j, position T_j, and width W_j values of the $J=3$ inner waves.

first relative minimum of $\tilde{x}'_{i,j}(n)$ for which $\tilde{x}_{i,j}(n_{E_j}) > A_P$ is fulfilled ensuring that the j:th inner wave can be defined.

Figure 2 illustrates a block diagram with the PDA steps.

B. Pulse waveform characteristics

Several morphological features associated with systolic arterial pressure and vascular compliance measures are extracted from each PDA based modeled PPG pulse. The amplitude $A_j(i)$ and the position $T_j(i)$ of an inner wave are defined as the amplitude and the position of the absolute maximum of $x_{i,j}(n)$, respectively. The width of $x_{i,j}(n)$, denoted by $W_j(i)$, is estimated by the full-width at half maximum.

The time delay between the position of the main wave and the first reflected wave $T_{12} = T_2 - T_1$ as well as the percentage of amplitude loss in the first reflection $A_{12} = 100 \cdot (A_1 - A_2)/A_1$ are calculated (the dependence of i is omitted for simplicity). Similarly, T_{13} and A_{13} are calculated for the second reflected wave. The position T_1 and the width W_1 of the main wave are also subjected to analysis. Finally, the instantaneous HR is calculated using the fiducial points $n_F(i)$. Figure 3 shows an example of pulse waveform characteristics. The pulse-to-pulse interval for the pulses that were considered in PDA is given by $T_{BB}(i) = (n_B(i+1) - n_B(i))/F_s$.

In this study, distorted pulses are discarded. They are considered as such when at least one of the following criteria are satisfied: (a) the pulse wave is decomposed to less than 3 waves, (b) the amplitude of the main wave is not the largest of the three waves, i.e., $A_2 > A_1$ or $A_3 > A_1$, (c) the second wave is located at the end of the pulse interval, i.e., $T_2 > 0.8T_{BB}$, or (d) the third wave occurs earlier than $0.35T_{BB}$, i.e., $T_3 < 0.35T_{BB}$. For each feature, outlier rejection is complemented with a median absolute deviation (MAD)-based rule [27]; the threshold is defined as 5 times the running MAD of the previous 50 pulses.

C. Statistical analysis

The median value of a pulse waveform characteristic is obtained for each subject and condition C, $C \in \{\mathcal{B}, \mathcal{S}_T, \mathcal{S}_C, \mathcal{R}\}$. In this study, only the first 5 minutes of $\mathcal{B}$ are taken into account since the time required for filling the psychometric tests can differ among subjects or groups.

Individual differences are assessed separately for HC and MDD group. A non-parametric Friedman test of differences among repeated measures is conducted for evaluating the individual differences across the stages of the experimental protocol. To identify which data come from a different distribution, a multi-comparison test (post hoc analysis) with Bonferroni correction is carried out using the paired t-test, and the Wilcoxon signed rank test when appropriate.

Differences in autonomic reactivity between MDD patients and HC subjects are assessed using the Cohen's d parameter and the area under the curve (AUC) of the receiver operating characteristic curve, which measure the size of an effect (depression) and the degree of separability between groups, respectively. The intra-subject difference of a feature $\mathcal{F}$, $\mathcal{F} \in \{\text{HR}, W_1, T_1, T_{12}, T_{13}, A_{12}, A_{13}\}$, between two conditions C_1 and C_2, denoted as $\Delta(\mathcal{F})_{C_1}^{C_2}$, is used as an index of autonomic reactivity. The reactivity indices are calculated by subtracting the value of the feature $\mathcal{F}$ in C_1 from C_2. The changes from basal to stress, from stress to recovery or from basal to recovery stage are studied for assessing autonomic reactivity.

Correlation (Pearson) analyses are carried out for testing bivariate associations between the most significant autonomic reactivity indices and depression severity scores assessed either with HDRS or BDI scores. Differences in demographic data between groups are assessed with the t-test for independent samples, and the Mann-Whitney U non-parametric test

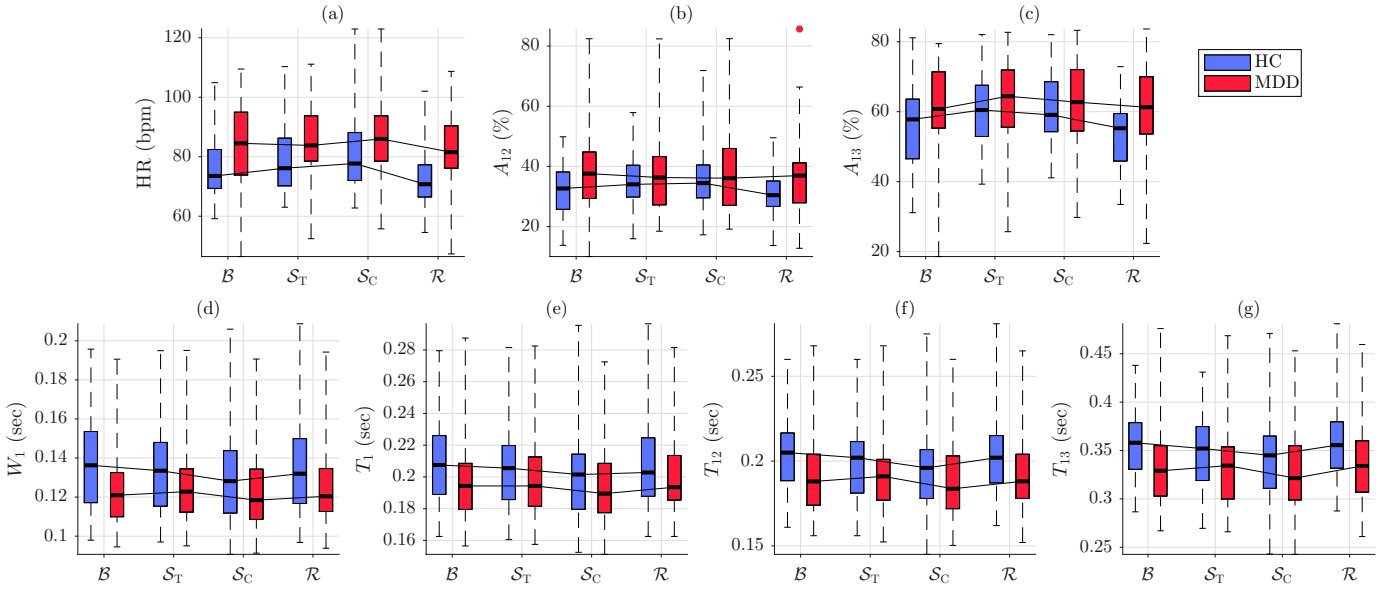

Fig. 4. Functional boxplots of pulse waveform characteristics. (a) Heart rate (HR), (b) percentage of amplitude loss in the first reflection (A_{12}), (c) percentage of amplitude loss in the second reflection (A_{13}), (d) width of the main wave (W_1), (e) time occurrence of the main wave (T_1), (f) time delay between the main wave and the first reflected wave (T_{12}), and (g) time delay between the main wave and the second reflected wave (T_{13}). The group of HC and MDD subjects are marked in blue and red, respectively.

when appropriate. The significance threshold in this study is set to $p < 0.01$.

IV. Results

The percentage (mean±SD) of discarded pulses for each stage was $2.3\% \pm 4.8\%$ ($\mathcal{B}$), $4.4\% \pm 6.6\%$ ($\mathcal{S}_T$), $4.0\% \pm 6.7\%$ ($\mathcal{S}_C$), and $3.6\% \pm 5.7\%$ ($\mathcal{R}$) suggesting that few distorted pulses are present in the PPG recordings. The number of analyzed pulses (mean±SD) was 370 ± 102 ($\mathcal{B}$), 262 ± 137 ($\mathcal{S}_T$), 317 ± 105 ($\mathcal{S}_C$), and 369 ± 102 ($\mathcal{R}$).

As can be seen from the boxplots in Fig. 4, patients with depression show higher values of HR and vascular compliance-related parameters A_{12} and A_{13} compared to healthy controls. In contrast to that, the healthy controls show higher values for the pulse transit time surrogates T_{12} and T_{13} and the temporal parameters related to the main wave, i.e, W_1 and T_1.

Friedman tests indicated that there are statistically significant differences in HR and A_{13} for both groups, while only the HC group showed significant differences in the rest of parameters across the different stages. The post hoc analysis revealed which stage in particular differs from each other. Table II illustrates the statistical significance of the multi-comparison paired tests. Results show that HC subjects exhibit statistical differences in all characteristics during the verbal stressor compared either to basal ($\mathcal{B}$ vs $\mathcal{S}_C$) or to recovery stage ($\mathcal{S}_C$ vs $\mathcal{R}$). On the other hand, statistically significant ($p<0.001$) individual differences were found in MDD patients mainly for HR and A_{13} indices, which were associated with changes from stress to recovery, i.e., $\mathcal{S}_T$ vs $\mathcal{R}$ and $\mathcal{S}_C$ vs $\mathcal{R}$. An example of average pulse waveforms for a HC and a MDD subject (matched by sex, age and BMI) is shown in Fig. 5. For each stage, prior to averaging operation, the pulses are aligned to the position of the pulse start (basal point). This figure highlights the fact that across different stages within the same subject minimal changes of waveform characteristics, including HR, T_{13}, and A_{13}, are observed for the MDD compared to the HC subject.

TABLE II
Statistical significance of HC / MDD individual differences along different stages

	$\mathcal{B}$ vs $\mathcal{S}_T$	$\mathcal{B}$ vs $\mathcal{S}_C$	$\mathcal{B}$ vs $\mathcal{R}$	$\mathcal{S}_T$ vs $\mathcal{R}$	$\mathcal{S}_C$ vs $\mathcal{R}$
HR	** / n.s.	** / n.s.	** / *	** / **	** / **
W_1	n.s. / n.s.	** / n.s.	n.s. / n.s.	n.s. / n.s.	** / n.s.
T_1	n.s. / n.s.	** / n.s.	n.s. / n.s.	n.s. / n.s.	** / n.s.
T_{12}	n.s. / n.s.	** / n.s.	n.s. / n.s.	n.s. / n.s.	** / n.s.
T_{13}	n.s. / n.s.	** / n.s.	n.s. / n.s.	n.s. / n.s.	** / *
A_{12}	* / n.s.	** / n.s.	n.s. / n.s.	** / n.s.	** / n.s.
A_{13}	* / *	* / n.s.	** / n.s.	** / **	** / **

* $p < 0.01$, ** $p < 0.001$, n.s. not significant

Results of the differences in autonomic reactivity between MDD and HC subjects are summarized in Table III. Results show that the amplitude loss in the second A_{13} reflection is associated with larger effect sizes compared to HR or other pulse waveform characteristics. A higher degree of separability between groups is observed when changes from either basal ($\mathcal{B}$) or stressful stages ($\mathcal{S}_T$, $\mathcal{S}_C$) to recovery phase ($\mathcal{R}$) are considered, yielding AUC values of 0.72, 0.77, and 0.74 for $\Delta(A_{13})^{\mathcal{B}}_{\mathcal{R}}$, $\Delta(A_{13})^{\mathcal{S}_T}_{\mathcal{R}}$ $\Delta(A_{13})^{\mathcal{S}_C}_{\mathcal{R}}$, respectively.

The results of the correlation analysis in Table IV indicate that there is a statistically significant negative correlation between depression severity scores and autonomic reactivity indices. Comparing the results between the most promising features, it can be seen that $\Delta(A_{13})^{\mathcal{S}_C}_{\mathcal{R}}$ is associated with higher (absolute) correlation values; $r = -0.50$ and $r = -0.43$ for HDRS and BDI scores, respectively. Note that depression severity scores are transformed using the squared root (log transformation is avoided due to zeros in HDRS) to increase the linear relationship with the autonomic reactivity indices.

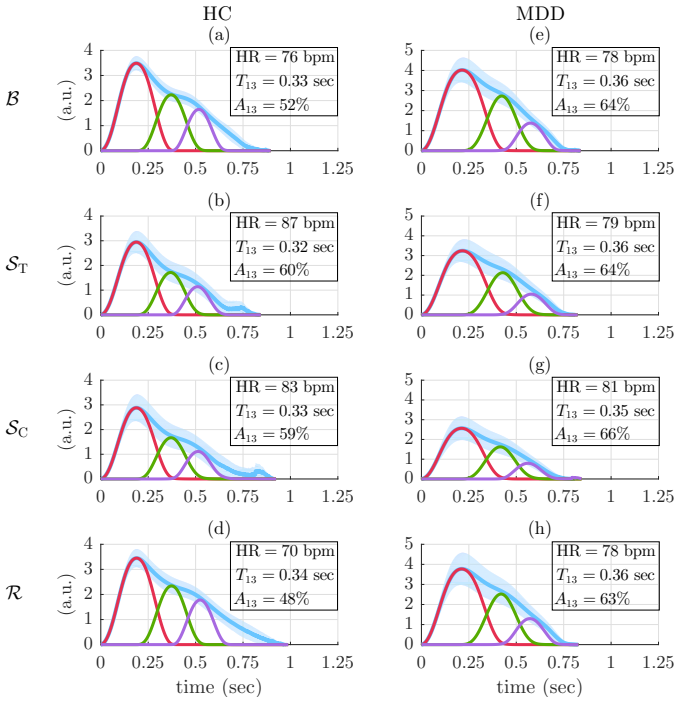

Fig. 5. Average pulse waveforms for two subjects. Average pulse waveforms for (a)-(d) a HC, and (e)-(h) a MDD subject. Each row corresponds to one of the experimental protocol stages, i.e., $\mathcal{B}$, $\mathcal{S}_T$, $\mathcal{S}_C$, and $\mathcal{R}$. The blue lines and shaded areas represent the ensemble average and standard deviation, respectively, while the ensemble average for the three inner waves are marked with red, green, and purple lines. The waveform characteristics HR, T_{13}, and A_{13} are illustrated at the top right of each graph.

TABLE III
AUC / COHEN'S d VALUES OF AUTONOMIC REACTIVITY INDICES BETWEEN MDD AND HC GROUP

$\mathcal{F}$	$\Delta(\mathcal{F})^{\mathcal{S}_T}_{\mathcal{B}}$	$\Delta(\mathcal{F})^{\mathcal{S}_C}_{\mathcal{B}}$	$\Delta(\mathcal{F})^{\mathcal{B}}_{\mathcal{R}}$	$\Delta(\mathcal{F})^{\mathcal{S}_T}_{\mathcal{R}}$	$\Delta(\mathcal{F})^{\mathcal{S}_C}_{\mathcal{R}}$
HR	0.65 / -0.51	0.65 / -0.53	0.57 / -0.24	0.69 / -0.67	**0.71 / -0.67**
W_1	0.66 / 0.51	**0.70 / 0.61**	0.59 / -0.17	0.59 / 0.26	0.62 / 0.48
T_1	0.64 / 0.50	**0.70 / 0.62**	0.61 / -0.29	0.54 / 0.16	0.59 / 0.42
T_{12}	0.65 / 0.57	**0.72 / 0.66**	0.55 / -0.11	0.62 / 0.37	0.67 / 0.61
T_{13}	0.64 / 0.56	0.65 / 0.55	0.52 / 0.06	0.62 / 0.51	0.67 / 0.59
A_{12}	0.68 / -0.60	**0.70 / -0.60**	0.51 / -0.07	0.67 / -0.58	0.67 / -0.60
A_{13}	0.56 / -0.35	0.58 / -0.35	**0.72 / -0.68**	**0.77 / -0.85**	**0.74 / -0.81**

Note: in bold are marked the indices with AUC > 0.7

Figure 6 shows the scatter plots of $\sqrt{\text{HDRS}}$ and $\Delta(A_{13})$ pairs together with the line of best fit (least-squares minimization).

V. DISCUSSION

The present paper investigates the differences in autonomic reactivity to mental stress between MDD and healthy subjects by measuring changes in PPG morphology. The response to stress, induced by verbal and non-verbal cognitive tasks, is evaluated by means of PDA.

The intra-subject difference of PDA-derived features between two conditions, e.g., basal and stress, are considered as indices of autonomic reactivity. Results show that the stress response of MDD compared to HC subjects is different (Table III). Changes in PPG morphology quantified by $\Delta(A_{13})$ show a higher degree of separability between groups, i.e., larger AUC values, compared to all the indices considered

TABLE IV
CORRELATION COEFFICIENT r BETWEEN DEPRESSION SEVERITY SCORES AND AUTONOMIC REACTIVITY INDICES

	$\Delta(\mathcal{F})^{\mathcal{B}}_{\mathcal{R}}$	$\Delta(\mathcal{F})^{\mathcal{S}_T}_{\mathcal{R}}$	$\Delta(\mathcal{F})^{\mathcal{S}_C}_{\mathcal{R}}$
$r(\sqrt{\text{HDRS}}, \Delta(\text{HR}))$	-0.09	-0.39**	-0.40**
$r(\sqrt{\text{HDRS}}, \Delta(A_{12}))$	-0.01	-0.33*	-0.37*
$r(\sqrt{\text{HDRS}}, \Delta(A_{13}))$	-0.37**	-0.45**	-0.50**
$r(\sqrt{\text{BDI}}, \Delta(\text{HR}))$	-0.07	-0.34*	-0.31*
$r(\sqrt{\text{BDI}}, \Delta(A_{12}))$	0.05	-0.27*	-0.30*
$r(\sqrt{\text{BDI}}, \Delta(A_{13}))$	-0.33*	-0.43**	-0.43**

* $p < 0.01$, ** $p < 0.001$

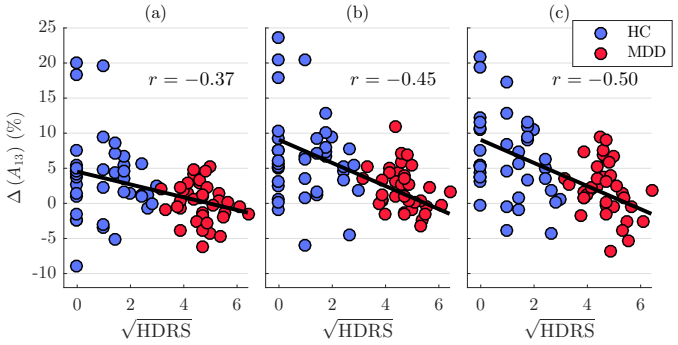

Fig. 6. Scatter plot of depression severity scores assessed with HDRS and autonomic reactivity index $\Delta(A_{13})$ for all subjects. (a) $\Delta(A_{13})^{\mathcal{B}}_{\mathcal{R}}$, (b) $\Delta(A_{13})^{\mathcal{S}_T}_{\mathcal{R}}$, and (c) $\Delta(A_{13})^{\mathcal{S}_C}_{\mathcal{R}}$. Least-squares reference lines are superimposed on the scatter plots. Correlation coefficients between depression severity scores and autonomic reactivity indices are displayed at the top right of each graph. The group of HC and MDD subjects are marked in blue and red, respectively.

in the study. This implies that vascular characteristics could provide complementary information about autonomic function.

Elevated HR values and increased amplitude loss in wave reflections, e.g. A_{13}, are observed during stress conditions (Fig. 4(a)-(c)) and they are associated with higher levels of sympathetic activity. Acute mental stress may increase aortic stiffness [28]. An increased arterial stiffness implies that the stroke volume flows through the arterial system and peripheral tissues mainly during systole due to the reduced distensibility of the elastic arteries and the aorta [29]. This causes both a larger peak in systolic part and a larger decline during diastolic part. Thus, an increment of A_{13} values during stressful tasks can be related to the inverse relationship between systolic (increased) and diastolic blood pressure (decreased).

An increased vagal tone following the stress induction may enhance differences in ANS regulation between MDD and HC subjects taking into consideration that $\Delta(A_{13})$ indices (Table III) yielded to large effect sizes, i.e., $|d| > 0.8$. On the contrary, changes in autonomic reactivity from basal to stress show lower AUC and effect sizes compared to changes from stress to recovery. These results are suggestive of a higher sympathetic tone in $\mathcal{B}$ compared to $\mathcal{R}$ stage. Filling psychometric tests, during $\mathcal{B}$ stage, does not imply a cognitive stressor, but it may require the attention and effort of the subject, which could affect the ANS state. Indeed, statistically significant (Table II) lower values of HR and A_{13} are observed for HC subjects in $\mathcal{R}$ compared to $\mathcal{B}$ (Fig. 4(a) and 4(c)).

Furthermore, a higher degree of depression is associated

with a decreased autonomic reactivity. The autonomic reactivity indices and depression severity scores are negatively correlated (Table IV). Taking into account that the range of depression severity scores (Fig. 6) covers all types of depressive symptoms (mild, moderate, severe, and very severe), stress response quantified by dynamic changes in vascular characteristics might be useful for depression monitoring. Blunted autonomic reactivity to stress might reflect suboptimal functioning of the cortical and limbic brain regions that are involved in motivation and cognitive ability [30]. Thus, deviations from an optimal response, in the face of challenge, may indicate that MDD patients are less capable than healthy subjects, to adjust their mental state to abrupt behavioral changes.

These results are in agreement with previous studies which showed that patients with depression are associated with blunted cardiovascular reactivity to psychological stressors. Reduced HR and systolic blood pressure reactivity during a speech task and less HR recovery in depressed patients compared to healthy control subjects was reported in [31]. Other studies pointed out that high scores of depression or anxiety symptomatology are associated with blunted blood pressure and HR reactivity to psychological stressors [32], [33].

Decreased autonomic reactivity in depression has been documented in a growing number of studies using HRV indices [34], [35]. Moreover, joint analyses of respiration and HRV showed less stressor-induced suppression of cardiac parasympathetic activity in MDD patients compared to healthy subjects [36]. In [37], entropy measures of cardiorespiratory coupling showed an increasing trend with depression severity.

Although PPG signal has been widely used for quantifying mental stress [38]–[40], few studies have explored the ability of PPG-derived indices to assess autonomic reactivity in MDD patients. It should be noted that short-term variability is often overestimated by PRV and, in addition, it has been reported that some mental stressors reduce the accuracy of PRV as a surrogate of HRV [41]–[43]. The PRV is affected by measurement errors related to lower accuracy of fiducial point detection, and physiological factors such as respiration [42]. Changes in respiratory patterns imposed by the exposure to stressful stimuli may mask the vagal withdrawal [44], [45].

One of the very few studies which analyzed morphological PPG features in MDD patients showed that entropy indices of systolic and diastolic amplitude of pulse waveform were positively correlated with suicidal score [17]. Higher entropy values imply a more uniform distribution of PPG amplitudes in depressed patients with suicidal ideation, fact that could be related to minimal changes in ANS state. Seldenrijk et al. [46] showed that the early wave reflection in depressive or anxiety disorders was associated with higher arterial stiffness, which agrees with the findings of the present study. Altered vasomotor tone in MDD patients, owing to the autonomic imbalance (increased sympathetic activity), has been related to changes in endothelial function, which is considered a gauge of vascular health [47]. Systematic reviews have shown that depressive symptoms are associated with subclinical atherosclerosis [48], [49]. Arterial stiffness may increase the risk for structural abnormalities in the mood regulatory centers of the brain due to small vessel lesions, contributing to the development of late-life depression (vascular depression hypothesis) [50]–[52]. Irrespective of whether depression is a cause or effect of arterial stiffness, impaired arterial compliance might constitute a biomarker of mental health and might contribute to the increased frequency of cardiovascular diseases observed in MDD patients [53], [54].

In [18], the PDA-based inner waves of a PPG pulse were modeled as Gaussian waves using a Trust-Region algorithm for the fitting procedure, while, in this work, waveform characteristics are derived from the inner waves without the use of fitting. Similar results (not shown) are obtained for both approaches, thereby suggesting a faster feature extraction, which seems appealing for a future integration of PDA into wearable devices. A low sampling frequency might be also required for implementation in wearables, however, it may produce a jitter in fiducial point estimation [55]. To reduce the effect of jitter, an algorithm of interpolation (up-sampling) is commonly used for refining the fiducial point [56]. Based on additional analyses (not shown), where the PPG signal $x_{\text{PPG}}(n)$ was up-sampled from $F_s = 250$ Hz to 1000 and 2000 Hz, the effect of F_s on morphological indices was minimal leading to changes in the order of 1% for AUC values. Although up-sampling is crucial in PRV analyses, since the effect of jitter can alter spectral indices considerably [57], PPG signals recorded at low sampling frequency, e.g. $F_s = 250$ Hz, may suffice for deriving morphological indices. Note also that if after up-sampling the same tendency for the raw values across conditions is observed, the study of individual differences through autonomic reactivity indices can be affected at even less extent. Further studies can be done by fusing information from different waveform characteristics to further improve the assessment of autonomic reactivity.

The main difference of the present technique with respect to other PDA techniques in the literature is that both main and reflected waves are assumed to be symmetrical and they are extracted one-by-one, instead of obtaining a modeled PPG by fitting several waves at once [58], [59]. This facilitates the interpretation of model parameters based on the pulse wave propagation physiology. Moreover, this decomposition is based on the hypothesis that half of the incidence pulse does not overlap with the reflected one, and same with the following pulses. However, in cases where fast propagation occurs, there might be overlapping between waves, but it should be minimum since it is an overlap of the maximum incident pulse with the lower tails of the reflected one. This point deserves a simulation study for evaluating hemodynamic responses to controlled fluxes, which, however, is out of the scope of this study.

A limitation of the present study is that the performance of PDA was studied mainly on a fingertip PPG signal. PPG signals recorded at different places on the body (wrist, forehead, ear) exhibit quite different morphologies from that of the fingers. Therefore, the current methodology can not be generalized automatically to all PPG signals. However, the database did not include PPG recordings at a second location on the body. Further studies, where PPG signals acquired from various sites of the body are available, should be conducted

for evaluating the effect of the recording site on the PDA performance.

Another limitation is that most of MDD patients were in antidepressant treatment. Results of a recent cross-sectional study have shown that there is no association between arterial stiffness and longitudinal exposure to antidepressants [60]. In [61], [62], it was found that depressed patients who responded to antidepressant treatment presented sustained improvement in vascular function. Moreover, in a large cohort study, Dregan et al. [63] showed that the association of depression with arterial stiffness in midlife was mediated via both metabolic syndrome and inflammatory processes rather than antidepressant medication. The hypothesized bidirectional relationship between depression and arterial stiffness can be also mediated by the lack of physical activity and poor diet, rather than the use of antidepressants [64], [65]. However, the reduced number of MDD patients without medication (3 out of 40, see Table I) do not allow the impact of drug treatment on pulse waveform characteristics to be assessed. Furthermore, there are also differences in medication (types, doses, and duration), due to the severity of the depressive symptoms, which further complicate such an analysis.

VI. Conclusions

In this study, the autonomic reactivity to stressful stimuli in patients with depression and healthy subjects is assessed by quantifying dynamic changes in PPG morphology using a pulse decomposition analysis. Results show that the stress response of MDD compared to healthy subjects is different and a decreased autonomic reactivity is associated with higher degree of depression. Vascular characteristics such as the percentage of amplitude loss in wave reflections have a potential to become digital biomarkers for the diagnosis and monitoring of depression.

VII. Acknowledgment

The computation was performed by the ICTS "NANBIOSIS", more specifically by the High Performance Computing Unit of the CIBER in Bioengineering, Biomaterials & Nanomedicine (CIBER-BBN) at the University of Zaragoza.

References

[1] W. H. Organization *et al.*, "Depression and other common mental disorders: global health estimates," World Health Organization, Tech. Rep., 2017.

[2] S. L. James *et al.*, "Global, regional, and national incidence, prevalence, and years lived with disability for 354 diseases and injuries for 195 countries and territories, 1990–2017: a systematic analysis for the Global Burden of Disease Study 2017," *The Lancet*, vol. 392, no. 10159, pp. 1789–1858, 2018.

[3] C. E. Angermann and G. Ertl, "Depression, anxiety, and cognitive impairment," *Curr. Heart. Fail. Rep.*, vol. 15, no. 6, pp. 398–410, 2018.

[4] A. Halaris, "Inflammation-associated co-morbidity between depression and cardiovascular disease," in *Inflammation-Associated Depression: Evidence, Mechanisms and Implications*. Springer, 2016, pp. 45–70.

[5] I. Granville Smith *et al.*, "Acute coronary syndrome and depression: a review of shared pathophysiological pathways," *Aust. N. Z. J. Psychiatry*, vol. 49, no. 11, pp. 994–1005, 2015.

[6] S. M. Monroe and A. D. Simons, "Diathesis-stress theories in the context of life stress research: Implications for the depressive disorders." *Psychol. Bull.*, vol. 110, no. 3, p. 406, 1991.

[7] J. Dean and M. Keshavan, "The neurobiology of depression: An integrated view," *Asian J. Psychiatr.*, vol. 27, pp. 101–111, 2017.

[8] P. Willner *et al.*, "The neurobiology of depression and antidepressant action," *Neurosci. Biobehav. Rev.*, vol. 37, no. 10, pp. 2331–2371, 2013.

[9] R. Gaspersz *et al.*, "Patients with anxious depression: overview of prevalence, pathophysiology and impact on course and treatment outcome," *Curr. Opin. Psychiatry*, vol. 31, no. 1, pp. 17–25, 2018.

[10] L. Carnevali *et al.*, "Autonomic and brain morphological predictors of stress resilience," *Front. Neurosci.*, vol. 12, p. 228, 2018.

[11] C. Osório *et al.*, "Adapting to stress: understanding the neurobiology of resilience," *Behav. Med.*, vol. 43, no. 4, pp. 307–322, 2017.

[12] C. Schiweck *et al.*, "Heart rate and high frequency heart rate variability during stress as biomarker for clinical depression. a systematic review," *Psychol. Med.*, vol. 49, no. 2, pp. 200–211, 2019.

[13] J. L. Hamilton and L. B. Alloy, "Atypical reactivity of heart rate variability to stress and depression across development: Systematic review of the literature and directions for future research," *Clin. Psychol. Rev.*, vol. 50, pp. 67–79, 2016.

[14] L. M. Holsen *et al.*, "Brain hypoactivation, autonomic nervous system dysregulation, and gonadal hormones in depression: a preliminary study," *Neurosci. Lett.*, vol. 514, no. 1, pp. 57–61, 2012.

[15] S. Dagdanpurev *et al.*, "Development and clinical application of a novel autonomic transient response-based screening system for major depressive disorder using a fingertip photoplethysmographic sensor," *Front. Bioeng. Biotechnol.*, vol. 6, 2018.

[16] J. Allen, "Photoplethysmography and its application in clinical physiological measurement," *Physiol. Meas.*, vol. 28, no. 3, p. R1, 2007.

[17] A. H. Khandoker *et al.*, "Suicidal ideation is associated with altered variability of fingertip photo-plethysmogram signal in depressed patients," *Front. Physiol.*, vol. 8, p. 501, 2017.

[18] J. Lázaro *et al.*, "Baroreflex sensitivity measured by pulse photoplethysmography," *Front. Neurosci.*, vol. 13, 2019.

[19] A. P. Association *et al.*, *Diagnostic and statistical manual of mental disorders (DSM-5®)*. American Psychiatric Pub, 2013.

[20] M. Hamilton, "A rating scale for depression," *J. Neurol. Neurosurg. Psychiatry*, vol. 23, no. 1, p. 56, 1960.

[21] A. T. Beck *et al.*, "Beck depression inventory-II," *San Antonio*, vol. 78, no. 2, pp. 490–498, 1996.

[22] A. Arza *et al.*, "Measuring acute stress response through physiological signals: towards a quantitative assessment of stress," *Med. Biol. Eng. Comput.*, vol. 57, no. 1, pp. 271–287, 2019.

[23] T. McMorris, "Chapter 1 - History of Research into the Acute Exercise–Cognition Interaction: A Cognitive Psychology Approach," in *Exercise-Cognition Interaction*, T. McMorris, Ed. San Diego: Academic Press, 2016, pp. 1–28.

[24] F. Scarpina and S. Tagini, "The stroop color and word test," *Front. Psychol.*, vol. 8, p. 557, 2017.

[25] P. Armanac *et al.*, "Cardiovascular changes induced by acute emotional stress estimated from the pulse transit time difference," in *2019 Computing in Cardiology (CinC)*. IEEE, 2019, pp. 1–4.

[26] J. Lázaro *et al.*, "Pulse rate variability analysis for discrimination of sleep-apnea-related decreases in the amplitude fluctuations of pulse photoplethysmographic signal in children," *IEEE J. Biomed. Health Inform.*, vol. 18, no. 1, pp. 240–246, 2013.

[27] R. Bailón *et al.*, "A robust method for ECG-based estimation of the respiratory frequency during stress testing," *IEEE Trans. Biomed. Eng.*, vol. 53, no. 7, pp. 1273–1285, 2006.

[28] C. Vlachopoulos *et al.*, "Acute mental stress has a prolonged unfavorable effect on arterial stiffness and wave reflections," *Psychosom. Med.*, vol. 68, no. 2, pp. 231–237, 2006.

[29] L. Zanoli *et al.*, "Arterial structure and function in inflammatory bowel disease," *World J. Gastroenterol.*, vol. 21, no. 40, p. 11304, 2015.

[30] D. Carroll *et al.*, "The behavioural, cognitive, and neural corollaries of blunted cardiovascular and cortisol reactions to acute psychological stress," *Neurosci. Biobehav. Rev.*, vol. 77, pp.74–86, 2017.

[31] K. Salomon *et al.*, "Major depressive disorder is associated with attenuated cardiovascular reactivity and impaired recovery among those free of cardiovascular disease." *Health Psychol.*, vol. 28, no. 2, p. 157, 2009.

[32] K. Yuenyongchaiwat *et al.*, "Symptoms of anxiety and depression are related to cardiovascular responses to active, but not passive, coping tasks," *Braz. J. Psychiatry*, vol. 39, no. 2, pp. 110–117, 2017.

[33] S. R. de Rooij *et al.*, "Depression and anxiety: Associations with biological and perceived stress reactivity to a psychological stress protocol in a middle-aged population," *Psychoneuroendocrinology*, vol. 35, no. 6, pp. 866–877, 2010.

[34] T. Shinba, "Altered autonomic activity and reactivity in depression revealed by heart-rate variability measurement during rest and task conditions," *Psychiatry Clin. Neurosci.*, vol. 68, no. 3, pp. 225–233, 2014.
[35] L. M. Bylsma *et al.*, "Rsa reactivity in current and remitted major depressive disorder," *Psychosom. Med.*, vol. 76, no. 1, p. 66, 2014.
[36] S. Kontaxis *et al.*, "Heart rate variability analysis guided by respiration in major depressive disorder," in *2018 Computing in Cardiology Conference (CinC)*, vol. 45. IEEE, 2018, pp. 1–4.
[37] L. Zhao *et al.*, "Cardiorespiratory coupling analysis based on entropy and cross-entropy in distinguishing different depression stages," *Front. Physiol.*, vol. 10, p. 359, 2019.
[38] G. Giannakakis *et al.*, "Review on psychological stress detection using biosignals," *IEEE Trans. Affect. Comput.*, 2019.
[39] P. H. Charlton *et al.*, "Assessing mental stress from the photoplethysmogram: a numerical study," *Physiol. Meas.*, vol. 39, no. 5, p. 054001, 2018.
[40] M. Rinkevičius *et al.*, "Photoplethysmogram signal morphology-based stress assessment," in *2019 Computing in Cardiology (CinC)*. IEEE, 2019, pp. 1–4.
[41] E. Gil *et al.*, "Photoplethysmography pulse rate variability as a surrogate measurement of heart rate variability during non-stationary conditions," *Physiol. Meas.*, vol. 31, no. 9, p. 1271, 2010.
[42] A. Schäfer and J. Vagedes, "How accurate is pulse rate variability as an estimate of heart rate variability?: A review on studies comparing photoplethysmographic technology with an electrocardiogram," *Int. J. Cardiol.*, vol. 166, no. 1, pp. 15–29, 2013.
[43] R. Pernice *et al.*, "Comparison of short-term heart rate variability indexes evaluated through electrocardiographic and continuous blood pressure monitoring," *Med. Biol. Eng. Comput.*, vol. 57, no. 6, pp. 1247–1263, 2019.
[44] A. Brugnera *et al.*, "Heart rate variability during acute psychosocial stress: A randomized cross-over trial of verbal and non-verbal laboratory stressors," *Int. J. Psychophysiol.*, vol. 127, pp. 17–25, 2018.
[45] M. X. Hu *et al.*, "Differential autonomic nervous system reactivity in depression and anxiety during stress depending on type of stressor," *Psychosom. Med.*, vol. 78, no. 5, pp. 562–572, 2016.
[46] A. Seldenrijk *et al.*, "Depression, anxiety, and arterial stiffness," *Biol. Psychiatry*, vol. 69, no. 8, pp. 795–803, 2011.
[47] E. A. Patvardhan *et al.*, "Assessment of vascular endothelial function with peripheral arterial tonometry: information at your fingertips?," *Cardiol. Rev.*, vol. 18, no. 1, pp.20–28, 2010.
[48] M. J. M. van Agtmaal *et al.*, "Association of microvascular dysfunction with late-life depression: a systematic review and meta-analysis," *JAMA Psychiatry*, vol. 74, no. 7, pp.729–739, 2017.
[49] Y. Wu *et al.*, "The relationship of depressive symptoms and functional and structural markers of subclinical atherosclerosis: A systematic review and meta-analysis," *Eur. J. Prev. Cardiol.*, vol. 25, no. 7, pp.706–716, 2018.
[50] W. D. Taylor *et al.*, "The vascular depression hypothesis: mechanisms linking vascular disease with depression," *Mol. Psychiatry*, vol. 18, no. 9, pp.963–974, 2013.
[51] G. F. Mitchell *et al.*, "Arterial stiffness, pressure and flow pulsatility and brain structure and function: the Age, Gene/Environment Susceptibility–Reykjavik study," *Brain*, vol. 134, no. 11, pp.3398–3407, 2011.
[52] T. T. van Sloten *et al.*, "Carotid artery stiffness and incident depressive symptoms: the Paris prospective study III," *Biol. Psychiatry*, vol. 85, no. 6, pp.498–505, 2019.
[53] V. Vaccarino *et al.*, "Depression and coronary heart disease: 2018 position paper of the ESC working group on coronary pathophysiology and microcirculation," *Eur. Heart J.*, vol. 41, no. 17, pp.1687–1696, 2020.
[54] J. K. Rybakowski *et al.*, "Impairment of endothelial function in unipolar and bipolar depression," *Biol. Psychiatry*, vol. 60, no. 8, pp.889–891, 2006.
[55] Task Force of the European Society of Cardiology *et al.*, "Heart rate variability: standards of measurement, physiological interpretation and clinical use," *Circulation*, vol. 93, pp.1043–1065, 1996.
[56] M. Merri *et al.*, "Sampling frequency of the electrocardiogram for spectral analysis of the heart rate variability," *IEEE Trans. Biomed. Eng.*, vol. 37, no. 1, pp.99–106, 1990.
[57] A. H. Khandoker *et al.*, "Comparison of pulse rate variability with heart rate variability during obstructive sleep apnea," *Med. Eng. Phys.*, vol. 33, no. 2, pp.204–209, 2011.
[58] M. Huotari *et al.*, "Photoplethysmography and its detailed pulse waveform analysis for arterial stiffness," *J. Mech. Mater. Struct.*, vol. 44, no. 4, pp. 345–362, 2011.
[59] D. Goswami *et al.*, "A new two-pulse synthesis model for digital volume pulse signal analysis," *Cardiovasc. Eng.*, vol. 10, no. 3, pp.109–117, 2010.
[60] Á. Camacho *et al.*, "Antidepressant use and subclinical measures of atherosclerosis: The multi-ethnic study of atherosclerosis (mesa)," *J. Clin. Pharmacol.*, vol. 36, no. 4, p. 340, 2016.
[61] N. Kokras *et al.*, "The effect of treatment response on endothelial function and arterial stiffness in depression. A prospective study," *J. Affect. Disord.*, vol. 252,, pp.190–200, 2019.
[62] P. Oulis *et al.*, "Reversal of increased arterial stiffness in severely depressed women after 6-week antidepressant treatment," *J. Affect. Disord.*, vol. 122, no. 1–2, pp.164–166, 2010.
[63] A. Dregan *et al.*, "Associations between depression, arterial stiffness, and metabolic syndrome among adults in the uk biobank population study: A mediation analysis," *JAMA Psychiatry*, 2020.
[64] A. Kandola *et al.*, "Depressive symptoms and objectively measured physical activity and sedentary behaviour throughout adolescence: a prospective cohort study," *Lancet Psychiatry*, vol. 7, no. 3, pp.262–271, 2020.
[65] M. Gottsäter *et al.*, "Non-hemodynamic predictors of arterial stiffness after 17 years of follow-up: the Malmö Diet and Cancer study," *J. Hypertens.*, vol. 33, no. 5, p.957, 2015.